

Characterization of $(\text{Zr}_{1-x}\text{Ce}_x)_{0.84}\text{Y}_{0.16}\text{O}_{2-\delta}$ ceramics ($0 \leq x \leq 0.1$) derived by a wet chemical route

T. S. ZHANG*, J. MA, Y. Z. CHEN

School of Materials Engineering, Nanyang Technological University, Nanyang Avenue, Singapore 639798
E-mail: tszhang@ntu.edu.sg

S. H. CHAN

School of Mechanical and Production Engineering, Nanyang Technological University, Nanyang Avenue, Singapore 639798

Solid oxide fuel cells (SOFC) are very attractive because of high efficiency of energy conversion and low emission of pollutants. Doped zirconia ceramics are typically used as electrolytes for use in SOFCs due to their mechanical integrity and stability in both the reducing and oxidizing atmospheres. However, high manufacturing and maintenance costs arising from high operation temperature ($>900^\circ\text{C}$) of doped zirconia electrolytes limit their practical application [1, 2]. In recent years, doped ceria solid solutions with high ionic conductivities have been considered as promising electrolytes for use in intermediate-temperature SOFCs (IT-SOFC) [3, 4]. Unfortunately, a number of disadvantages are associated with the use of doped ceria electrolytes. They not only have a significantly weak mechanical strength, but are also less stable in reducing atmosphere.

Many attempts have been made to overcome the disadvantages of the ceria electrolytes. One of these approaches is to use composite technique based on doped ceria (e.g., $\text{Ce}_{0.8}\text{Gd}_{0.2}\text{O}_{2-\delta}$, CGO20) and doped zirconia (e.g., $\text{Zr}_{0.84}\text{Y}_{0.16}\text{O}_{2-\delta}$, YSZ) [5–10]. Unfortunately, these investigations have eventually proved to be unsuccessful. This is attributed to the fact that the true ceramic composites could not be obtained between CGO20 and YSZ since solid solutions will be formed between them at $>1300^\circ\text{C}$, leading to a significant decrease in ionic conductivities [6, 9, 11].

The present investigation is attempting to improve the ionic conductivity of YSZ electrolytes by small additions of CeO_2 (<10 at.%), which have received less attention in the literature. This is based on the following tentative idea. Since larger Ce^{4+} ions entering Zr^{4+} sites in YSZ crystallites causes an expansion of the unit cell, a larger channel radius through which an oxygen anion can move could be formed in $(\text{Zr}_{1-x}\text{Ce}_x)_{0.84}\text{Y}_{0.16}\text{O}_{2-\delta}$ ceramics, as compared to that in YSZ. As a result, a smaller association enthalpy for movement of oxygen anions is created in $(\text{Zr}_{1-x}\text{Ce}_x)_{0.84}\text{Y}_{0.16}\text{O}_{2-\delta}$ ceramics, thus leading to a high conductivity. On the other hand, the mechanical integrity and stability of the electrolytes are not expected to be weakened as the cerium content is low. The present study may also provide some references to the design of bilayer composite YSZ/CGO electrolytes.

The precursor powders of $(\text{Zr}_{1-x}\text{Ce}_x)_{0.84}\text{Y}_{0.16}\text{O}_{2-\delta}$ ceramics ($0 \leq x \leq 0.1$) were prepared via an oxalate coprecipitation method from high purity ($>99.9\%$) reagents $\text{ZrO}(\text{NO}_3)_2 \cdot 10\text{H}_2\text{O}$, $\text{Y}(\text{NO}_3)_3 \cdot 6\text{H}_2\text{O}$ and $\text{Ce}(\text{NO}_3)_3 \cdot 6\text{H}_2\text{O}$. The detailed preparation procedure can be found elsewhere [12]. The coprecipitates were washed several times using distilled water, then redispersed and washed twice in ethanol, finally dried at $\sim 100^\circ\text{C}$ for 20 hr. The precursor powders were calcined at 700°C for 3 hr, then ground in ethanol using a planetary milling system for 8 hr. The calcined powders were pressed at ~ 100 MPa into pellets using a die 10 mm diameter. The green pellets were sintered at 1400°C for 5 hr in air at a heating and cooling rate of $10^\circ\text{C}/\text{min}$.

The crystal phase was identified by X-ray diffraction (XRD) (Rigaku, Dmax-2200, Tokyo, Japan). The lattice parameters of the sintered samples were estimated from the XRD patterns using a software package provided by the Rigaku company. The densities of the sintered pellets were measured by the Archimedes method in a water bath. After polishing with fine emery papers, silver wires were attached on both sides of the pellets as electrodes at 850°C using silver paste. The ionic conductivity of the sintered pellets was measured in air using a two-probe impedance spectroscopy (Solartron 1260, UK), from 250 to 850°C and 1 to 10^7 Hz. A software package equipped with the instrument was used to separate the grain interior (GI) and the grain boundary (GB) contributions to the total conductivity.

The XRD patterns of $(\text{Zr}_{1-x}\text{Ce}_x)_{0.84}\text{Y}_{0.16}\text{O}_{2-\delta}$ ceramics with $x = 0, 0.01, 0.05,$ and 0.1 sintered at 1400°C for 5 hr are shown in Fig. 1, respectively, from which it can be seen that only single phase with fluorite-like structure could be detected, even in the ceramic with $x = 0.1$, indicating the formation of solid solutions from ZrO_2 , Y_2O_3 , and CeO_2 . It is also noted that the location of the XRD peaks moves towards the low-angle region as cerium content increases. This is because Ce^{4+} ion (0.97 nm) has a larger ionic size, as compared to Zr^{4+} ion (0.84 nm); and the dissolution of Ce^{4+} ions in YSZ crystallites will cause an expansion of unit cell. The calculated lattice parameter with cerium content is shown in Fig. 2. A nearly linear increase in

*Author to whom all correspondence should be addressed.

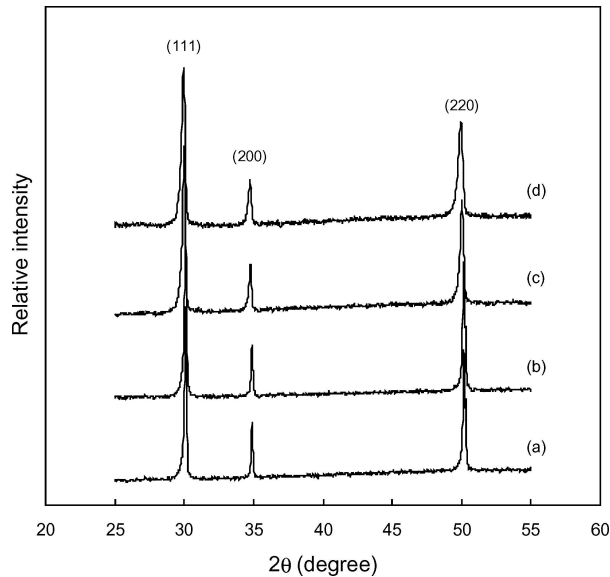


Figure 1 XRD patterns of $(Zr_{1-x}Ce_x)_{0.84}Y_{0.16}O_{2-\delta}$ ceramics sintered at 1400°C for 5 hr in air: (a) $x = 0$, (b) $x = 0.03$, (c) $x = 0.07$, and (d) $x = 0.1$.

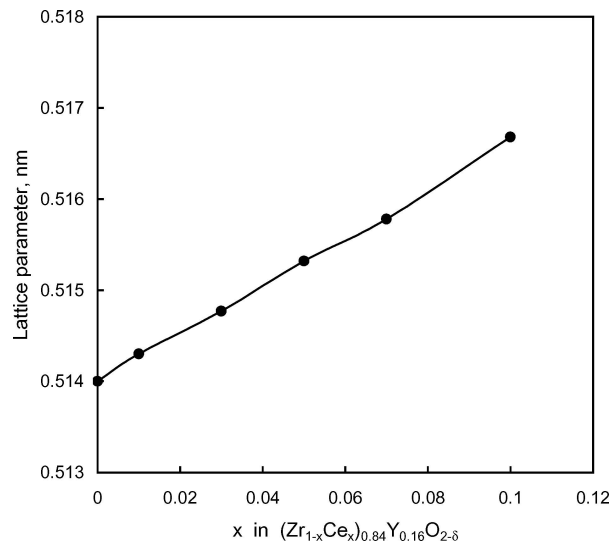


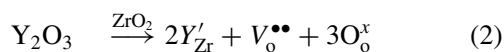
Figure 2 Lattice parameter vs. cerium content for $(Zr_{1-x}Ce_x)_{0.84}Y_{0.16}O_{2-\delta}$ ceramics sintered at 1400°C for 5 hr in air.

lattice parameter with increasing cerium content has been observed in cerium content range of $x = 0$ to 0.1 . This observation also confirms that CeO_2 completely dissolves into YSZ crystallites.

As revealed in Figs 1 and 2, the samples sintered at 1400°C for 5 hr are expected to form solid solution where both Y^{3+} and Ce^{4+} ions occupy Zr^{4+} sites, i.e.,



and



The theoretical densities of the solid solutions are calculated based on a modified Vacancy Model [13] as

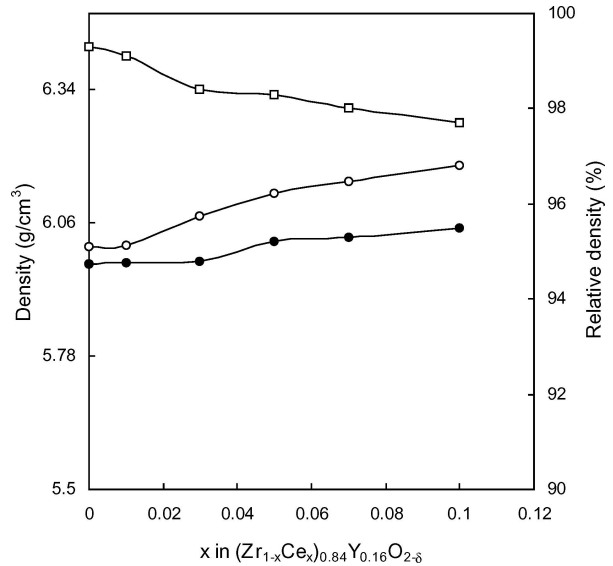


Figure 3 The measured density (●), theoretical density (○), and relative density (□) of $(Zr_{1-x}Ce_x)_{0.84}Y_{0.16}O_{2-\delta}$ ceramics.

follows:

$$d_{\text{th}} = \frac{4}{N_A a^3} \left\{ 0.84[(1-x)M_{\text{Zr}} + xM_{\text{Ce}}] + 0.16M_{\text{Y}} + \left(2 - \frac{1}{2} \times 0.16\right)M_o \right\} \quad (3)$$

where x is the Ce concentration ($0 \leq x \leq 0.1$), a is the lattice constant at room temperature of $(Zr_{1-x}Ce_x)_{0.84}Y_{0.16}O_{2-\delta}$ solid solutions as shown in Fig. 2, N_A is the Avogadro number, and M refers to the atomic weight. The theoretical and measured densities are shown in Fig. 3 for the $(Zr_{1-x}Ce_x)_{0.84}Y_{0.16}O_{2-\delta}$ solid solutions. It can be seen that although the sintered densities keep almost unchanged, the relative density decrease as cerium concentration increases. This is due to the fact that the theoretical densities increase with increasing cerium content. The above results suggest that the small additions of CeO_2 reduce the densification of the samples. Microstructural observations by scanning electron microscopy (SEM) also support the results obtained from the density measurement (no SEM micrographs are shown here). However, all the samples used have over 97% relative density.

The ionic conductivity of the samples was measured by means of a two-probe complex impedance analyzer. The interpretation of impedance data for polycrystalline materials, such as yttria-stabilized zirconia, has been well documented. $(Zr_{1-x}Ce_x)_{0.84}Y_{0.16}O_{2-\delta}$ ceramics ($0 \leq x \leq 0.1$) have typical impedance characteristics as could be found elsewhere [14]. The total (σ_t), grain interior (σ_{gi}) and grain boundary (σ_{gb}) conductivities could be obtained by fitting impedance data using a software package. Fig. 4 shows the conductivities for the $(Zr_{1-x}Ce_x)_{0.84}Y_{0.16}O_{2-\delta}$ ceramics measured at 450°C in air. Although the total, grain interior, and grain boundary conductivities all decrease as the cerium content increases, the decrease in the total conductivity results mainly from the contribution of grain-interior effect since the grain-boundary

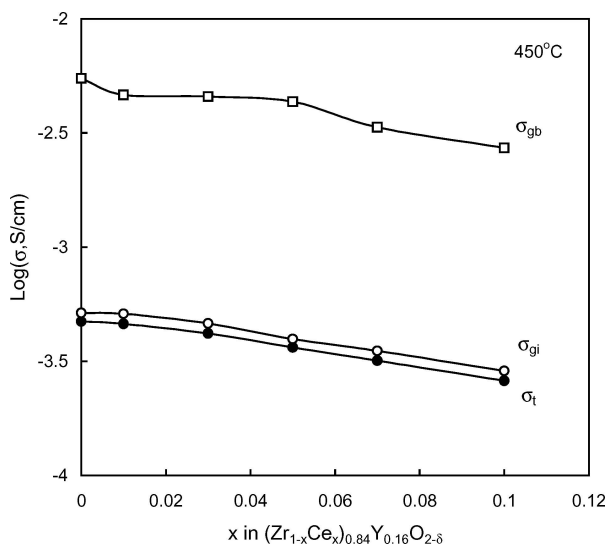


Figure 4 The total (σ_t), grain interior (σ_{gi}), and grain boundary (σ_{gb}) conductivities of $(Zr_{1-x}Ce_x)_{0.84}Y_{0.16}O_{2-\delta}$ ceramics, measured at 450°C in air.

conductivity is much high. The high grain-boundary conductivity of $(Zr_{1-x}Ce_x)_{0.84}Y_{0.16}O_{2-\delta}$ ceramics may be attributed to high purity precursors used, which contain less SiO_2 impurity. The above results are out of our expectation since no improved conductivity could be observed in the range of cerium content used, although the additions of cerium result in an expansion of unit cell (Fig. 2). Instead, the grain-interior conductivity decreases consistently with increasing cerium content. The results of Naito *et al.* [15] also demonstrated that the oxygen isotope diffusion coefficient decreases with cerium concentration in the Zr-rich region of the $[(ZrO_2)_{1-x}(CeO_2)_x]_{0.9}(Y_2O_3)_{0.1}$ ceramics. These re-

sults suggest that there may exist some unknown factors rather than the association enthalpy alone dominating the conduction behavior of $(Zr_{1-x}Ce_x)_{0.84}Y_{0.16}O_{2-\delta}$ ceramics ($0 \leq x \leq 0.1$).

References

1. N. Q. MINH, *J. Amer. Ceram. Soc.* **76** (1993) 563.
2. J. P. P. HUIJSMANS, *Curr. Opin. Solid State Mater. Sci.* **5** (2001) 317.
3. B. C. H. STEELE, *Solid State Ionics* **129** (2000) 95.
4. B. C. H. STEELE, in "Ceramic Oxygen Ion Conductors and Their Technological Application," edited by B. C. H. Steele (Institute of Materials, London, 1996) p. 103.
5. J. KIMPTON, T. H. RANDLE and J. DRENNAN, *Solid State Ionics* **149** (2002) 89.
6. J. LUO, R. J. BALL and R. STEVENS, *J. Mater. Sci.* **39** (2004) 235.
7. J. H. LEE, J. KIM, S. W. KIM, H. W. LEE and H. S. SONG, *Solid State Ionics* **166** (2004) 45.
8. H. ARASHI, H. NAITO and M. NAKATA, *Solid State Ionics* **76** (1995) 315.
9. T. S. ZHANG, H. T. HUANG, Z. Q. ZENG, P. HING and J. A. KINLER, *J. Mater. Sci. Lett.* **21** (2002) 1167.
10. A. TSOGA, A. NAOUMIDIS and D. STOVER, *Solid State Ionics* **135** (2000) 403.
11. K. EGUCHI, N. AKASAKA, H. MITSUYASU and Y. NONAKA, *ibid.* **135** (2000) 589.
12. K. HIGASHI, K. SONADA, H. ONO and S. SAMESHIMA, *J. Mater. Res.* **14** (1999) 957.
13. I. RIESS, D. BRAUNSHTEIN and D. S. TANNHAUSER, *J. Amer. Ceram. Soc.* **64** (1981) 479.
14. M. C. STEIL, F. THEVENOT and M. KLEITZ, *J. Electrochem. Soc.* **144** (1997) 192.
15. H. NAITO, N. SAKAI, T. OTAKE, H. YUGAMI and H. YOKOKAWA, *Solid State Ionics* **135** (2000) 669.

Received 26 October 2004

and accepted 18 February 2005